

Diffusion tensor imaging assesses white matter injury in neonates with hypoxic-ischemic encephalopathy

Hong-xin Li^{1,2}, Xing Feng^{1,*}, Qian Wang³, Xuan Dong⁴, Min Yu⁵, Wen-juan Tu²

1 Department of Neonatology, Children's Hospital of Soochow University, Suzhou, Jiangsu Province, China

2 Department of Neonatology, Changzhou Children's Hospital, Changzhou, Jiangsu Province, China

3 School of Biomedical Engineering, Shanghai Jiao Tong University, Shanghai, China

4 Department of Children's Health Research Center, Changzhou Children's Hospital, Changzhou, Jiangsu Province, China

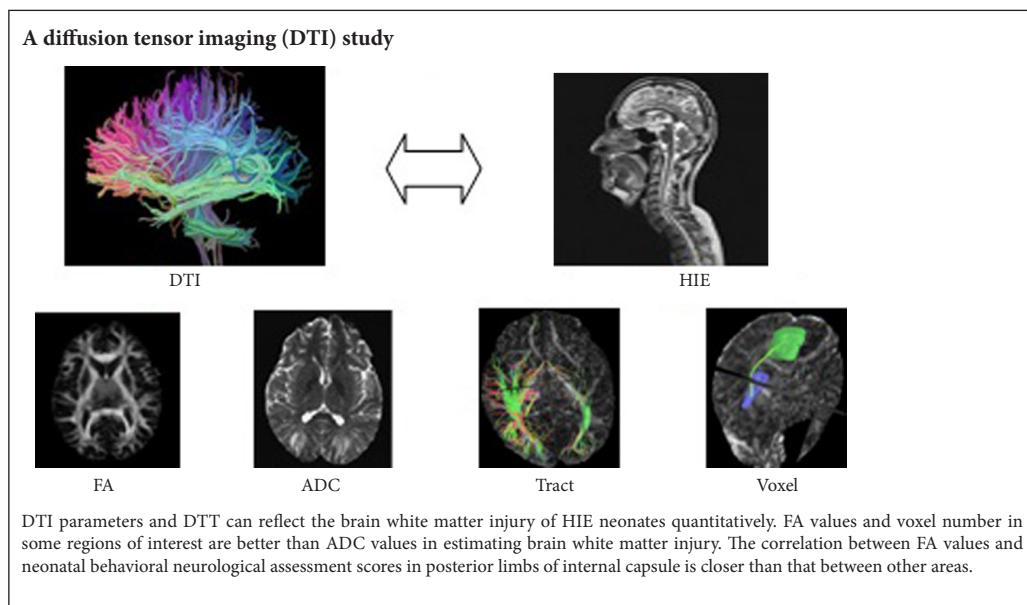
5 Nantong University, Nantong, Jiangsu Province, China

How to cite this article: Li HX, Feng X, Wang Q, Dong X, Yu M, Tu WJ (2017) Diffusion tensor imaging assesses white matter injury in neonates with hypoxic-ischemic encephalopathy. *Neural Regen Res* 12(4):603-609.

Open access statement: This is an open access article distributed under the terms of the Creative Commons Attribution-NonCommercial-ShareAlike 3.0 License, which allows others to remix, tweak, and build upon the work non-commercially, as long as the author is credited and the new creations are licensed under the identical terms.

Funding: This study was supported by a grant from the Clinical Medicine Science and Technology Projects in Jiangsu Province of China, No. BL2014037; a grant from the Changzhou City Science and Technology Support Plan in China, No. CE20165027; a grant from the Changzhou Health Development Planning Commission Major Projects in China, No. ZD201515; the Changzhou High-Level Health Personnel Training Project Funding.

Graphical Abstract



*Correspondence to:

Xing Feng, M.D.,
xing_feng66@hotmail.com.

orcid:

0000-0003-0519-3780
(Xing Feng)

doi: 10.4103/1673-5374.205102

Accepted: 2017-02-13

Abstract

With improvements in care of at-risk neonates, more and more children survive. This makes it increasingly important to assess, soon after birth, the prognosis of children with hypoxic-ischemic encephalopathy. Computed tomography, ultrasound, and conventional magnetic resonance imaging are helpful to diagnose brain injury, but cannot quantify white matter damage. In this study, ten full-term infants without brain injury and twenty-two full-term neonates with hypoxic-ischemic encephalopathy (14 moderate cases and 8 severe cases) underwent diffusion tensor imaging to assess its feasibility in evaluating white matter damage in this condition. Results demonstrated that fractional anisotropy, voxel volume, and number of fiber bundles were different in some brain areas between infants with brain injury and those without brain injury. The correlation between fractional anisotropy values and neonatal behavioral neurological assessment scores was closest in the posterior limbs of the internal capsule. We conclude that diffusion tensor imaging can quantify white matter injury in neonates with hypoxic-ischemic encephalopathy.

Key Words: nerve regeneration; fractional anisotropy; diffusion tensor imaging; apparent diffusion coefficient; voxel volume; neonatal behavioral neurological assessment; brain injury; white matter; neuroimaging; neural regeneration

Introduction

For many years, much attention has been given to improving the assessment of the prognosis of brain injury in hypoxic-ischemic encephalopathy (HIE) children. The incidence of HIE is still high (AbdelAziz, et al., 2017). The success rate of rescue in moderate and severe HIE has significantly improved (Pfister and Soll, 2010). Objective and sensitive indicators are needed to judge the prognosis. Head computed tomography (CT), ultrasound, and conventional magnetic resonance imaging (MRI) are helpful to diagnose brain injury, but cannot quantify the degree of white matter damage to arrive at a prognosis (Coleman et al., 2013; Jose et al., 2013; Duong and Watts, 2016). Conventional MRI reveals that the two kinds of brain injury in HIE children are basal ganglia and thalamic abnormalities and watershed damage, which are strongly associated with late motor and cognitive deficits (Okumura et al., 2008). However, children with obvious motor and cognitive abnormalities often have unremarkable scans (Aridas et al., 2014; Krishnan and Shroff, 2016). It is vital to find methodology capable of detecting white matter abnormalities in HIE children, who have a high risk of neurological sequelae. We explored the combined use of MRI and diffusion tensor imaging (DTI) to improve identification of CNS abnormalities.

DTI measures water molecule diffusion. It has great advantages in studying the integrity and orientation of white matter in normal and pathological states (Baldoli et al., 2015). Fractional anisotropy (FA) values and apparent diffusion coefficient (ADC) values in different brain regions can quantify the number and integrity of white matter fibers, detect white matter damage, and have been shown to dynamically visualize white matter repair (Pfefferbaum et al., 2014). DTI is a refinement of diffusion-weighted magnetic resonance imaging (DWI) (de Vries et al., 2011). A previous study showed that DWI in the acute stage of HIE (≤ 7 days) predicted the degree of brain damage; in the subacute stage (1–3 weeks), DWI showed pseudo-normalization, so DWI might underestimate the extent of damage to the basal ganglia and thalamus (Cavalleri et al., 2014). DTI is capable of applying a diffusion gradient magnetic field in at least six directions, can accurately determine the distribution of nerve fiber bundles and anisotropic characteristics of tissue, and is the best imaging method to reflect the structural integrity and directionality of white matter (Hüppi and Dubois, 2006). DTI has been used to study neuroregeneration and neurodegeneration, which have been confirmed by pathology or experimental results (Kim et al., 2015). It is thought that DTI can reflect HIE-induced white matter damage, and is certainly correlated with the severity of disease and prognosis (Lee et al., 2012). We also sought to assess the prognosis of neonatal HIE.

Subjects and Methods

Subjects

This was a cross-sectional study which was performed in the Changzhou Children's Hospital of China. Experiments were

conducted in accordance with the Approval of the Regional Ethics Review Boards of the Changzhou Children's Hospital (approval No. 20120019). The parents of patients signed informed consent. From January 2013 to December 2015, we recruited 22 full-term neonates with HIE (14 moderate cases and 8 severe cases; mostly with a history of neonatal asphyxia) and 10 full-term infants without brain injury (controls). The HIE patients were subdivided into moderate and severe groups. Patient baseline data are listed in **Table 1**. Diagnosis and inclusion criteria were in accordance with HIE diagnostic criteria and clinical classification of practical neonatal HIE, revised by Neonatology Group of the Chinese Pediatric Society of the Chinese Medical Association in Changsha, China in 2004 (The Subspecialty Group of Neonatology Pediatric Society Chinese Medical Association, 2005). The patients' conditions tended to be unstable in the first week, so MRI was conducted at the ages of 10–14 days. Patients with any of the following entities were excluded from the study: genetic metabolic diseases, central nervous system infection, congenital malformation of the brain, and chromosomal abnormality. Ten controls, including three cases of precipitate labor, four cases of scalp hematoma, two cases of cleft lip and palate, and one case of polydactyly, underwent MRI to exclude craniocerebral malformations. There was no significant difference in gestational age, mean weight or age on the day of examination among the three groups ($P > 0.05$) (**Table 1**).

MRI scan

All subjects were given 10% chloral hydrate 0.25–0.50 mL/kg by nasal feeding or enema, and subjected to scan after sleeping soundly. Scans were performed on a 3.0 T MRI scanner (Philips Achieva, Philips Inc., Rotterdam, the Netherlands) with a head matrix coil. Sequences were as follows: Fast low-angle shot (FLASH) T1-weighted images (T1WI), (repetition time 9.3 milliseconds, echo time 4.4 milliseconds, field of view 180 mm \times 180 mm, matrix 0.9 mm \times 0.9 mm, section thickness/intersection gap 4.5 mm/0.5 mm, number of excitations 2), turbo spin echo (TSE) T2-weighted images (T2WI) (repetition time 2,651 milliseconds, echo time 105 milliseconds \times 0.74 mm, section thickness/intersection gap 4.5 mm/0.5 mm, number of excitations 2), turbo inversion recovery magnitude (T2 TIRM) dark-fluid (repetition time 7,800 milliseconds, echo time 89 milliseconds, field of view 180 mm \times 180 mm, matrix 0.9 mm \times 1.1 mm, section thickness/intersection gap 4.5 mm/0.5 mm, number of excitations 2). DTI used scanning with a single-shot, spin-echo, echo-planar sequence (repetition time 4,104 milliseconds, echo time 60 milliseconds, field of view 180 mm \times 180 mm, matrix 1.8 mm \times 1.8 mm, b value 1,000 seconds/mm², diffusion sensitive gradient direction (diffusion directions) for 12, section thickness/intersection gap 2 mm/0 mm, incentive times 4). The scan baseline and the number of scan layers were the same for all sequences.

Image processing

The patients' imaging data were preprocessed. FSL software

Table 1 Baseline characteristics of HIE and control participants

Item	Control	Moderate HIE	Severe HIE	F/χ^2	P
Number	10	14	8		
Gestational age (week)	39.4±2.2	40.3±2.8	39.1±2.9	1.224	> 0.05
Weight (g)	3,084±370	3,367±480	3,167±340	1.001	> 0.05
Age at DTI (day)	15.9±5.1	16.3±4.4	14.3±4.9	1.142	> 0.05

HIE: Hypoxic-ischemic encephalopathy; DTI: diffusion tensor imaging.

Table 2 ADC values ($\times 10^{-3} \text{ mm}^2/\text{s}$) in different brain areas of normal, moderate, and severe HIE patients

	Control ($n = 10$)	Moderate HIE ($n = 14$)	Severe HIE ($n = 8$)	F	P
Corticospinal tract					
Left	1.16±0.04	1.18±0.08	1.15±0.06	9.32	> 0.05
Right	1.17±0.04	1.19±0.06	1.23±0.09	8.46	> 0.05
Cingulate gyrus					
Left	1.31±0.04	1.32±0.06	1.29±0.11	10.01	> 0.05
Right	1.25±0.04	1.26±0.08	1.23±0.04	9.25	> 0.05
SLF					
Left	1.23±0.04	1.22±0.06	1.39±0.11	9.11	> 0.05
Right	1.25±0.04	1.24±0.08	1.23±0.04	9.45	> 0.05
ALIC					
Left	1.26±0.04	1.36±0.08	1.22±0.10	7.35	> 0.05
Right	1.78±0.04	1.32±0.04	1.25±0.06	8.68	> 0.05
PLIC					
Left	1.19±0.09	1.29±0.13	1.19±0.08	7.98	> 0.05
Right	1.13±0.08	1.23±0.07	1.15±0.07	8.55	> 0.05
IFOF					
Left	1.15±0.05	1.19±0.08	1.14±0.10	9.12	> 0.05
Right	1.19±0.03	1.16±0.05	1.15±0.03	7.11	> 0.05
Thalamus					
Left	1.15±0.08	1.14±0.10	1.16±0.10	9.02	> 0.05
Right	1.16±0.05	1.15±0.03	1.16±0.09	7.17	> 0.05

Data are expressed as the mean ± SD, and analyzed by F -test. SLF: Superior longitudinal fasciculus; ALIC: anterior limbs of internal capsule; PLIC: posterior limbs of internal capsule; IFOF: inferior fronto-occipital fasciculus; HIE: hypoxic-ischemic encephalopathy.

(The Mathworks, Natick, MA, USA) was used for skull stripping. The Johns Hopkins White Matter Parcellation Atlas Type II (JHU-WMPM) atlas was registered with a particular patient image. The patient-specific image was segmented using the atlas' anatomical information. FA and ADC values in different areas of the specific patient images were calculated. b0, ADC, FA, and diffusion tensor tractography (DTT) diagrams were automatically generated with Neur03D software (The Mathworks). Twenty regions of interest (ROIs), including bilateral parietal cortex, deep white matter of the frontal lobe, anterior and posterior limbs of internal capsule, genu and splenium of corpus callosum, head of caudate nucleus, lenticular nucleus, thalamus, and pons, were selected in the b0 diagram. These ROIs were generated automatically, and were normalized with a neonatal model. Data were input into the software (DTI studio, Wellcome Department of Cognitive

Table 3 FA values in different brain areas of normal, moderate, and severe HIE patients

	Control ($n = 10$)	Moderate HIE ($n = 14$)	Severe HIE ($n = 8$)	F	P
Corticospinal tract					
Left	0.36±0.14	0.35±0.08	0.31±0.12	1.33	> 0.05
Right	0.39±0.14	0.33±0.11	0.30±0.13	1.56	> 0.05
Cingulate gyrus					
Left	0.33±0.11	0.32±0.06	0.49±0.11	1.11	> 0.05
Right	0.25±0.14	0.24±0.08	0.23±0.11	1.45	> 0.05
SLF					
Left	0.33±0.12	0.32±0.16	0.29±0.11	2.33	> 0.05
Right	0.25±0.11	0.24±0.18	0.23±0.14	2.78	> 0.05
ALIC					
Left	0.26±0.04	0.25±0.08	0.22±0.10	1.45	> 0.05
Right	0.38±0.04	0.32±0.04	0.25±0.06	1.88	> 0.05
PLIC					
Left	0.59±0.09	0.39±0.13*	0.19±0.08#	5.18	< 0.05
Right	0.63±0.08	0.53±0.07*	0.15±0.07#	5.55	< 0.05
IFOF					
Left	0.35±0.15	0.34±0.08	0.24±0.10	2.12	> 0.05
Right	0.39±0.13	0.36±0.15	0.25±0.03	2.11	> 0.05
Thalamus					
Left	0.54±0.08	0.34±0.10*	0.24±0.10#	4.12	< 0.05
Right	0.56±0.15	0.35±0.13*	0.15±0.03#	5.11	< 0.05

Data are expressed as the mean ± SD, and analyzed by F -test. * $P < 0.05$, vs. control group; # $P < 0.05$, vs. moderate HIE group. SLF: Superior longitudinal fasciculus; ALIC: anterior limbs of internal capsule; PLIC: posterior limbs of internal capsule; IFOF: inferior fronto-occipital fasciculus; HIE: hypoxic-ischemic encephalopathy.

Neurology, London, UK) for automatic generation of ADC and FA values. Each ROI was $10 \pm 2 \text{ mm}^2$. ROIs were placed within each measured structure according to its contour to avoid partial volume effects or adjacent structures.

Prognostication

The neonatal behavioral neurological assessment (NBNA) score (Bao, 1995) was calculated at age 15 days by a doctor. The content of NBNA (5 parts 20 items) includes behavioral ability (6), active and passive muscle tension (8 and 4, respectively), primitive reflex (3) and evaluation of general condition (3) for a total of 20 items, each item being scored 0, 1, or 2. Infants scoring > 35 were graded as "normal," and those with a score < 35 were graded as "abnormal." All patients were assessed at an ambient temperature of 24–28 °C in dim light and in a quiet environment. Each check was completed within 10 minutes.

Statistical analysis

The data, expressed as the mean ± SD, were analyzed with SPSS 17.0 software (SPSS, Chicago, IL, USA). The F -test was used to analyze DTI parameters, including ADC and FA values in the ROIs, and voxel volume, as well as the integrity and quantity of white matter fibers in DTT images, among the three groups. FA values and NBNA scores were analyzed

Table 4 Voxel volume in different brain areas of normal, moderate, and severe HIE patients

	Control (n = 10)	Moderate HIE (n = 14)	Severe HIE (n = 8)	F	P
Corticospinal tract					
Left	299±112	236±87	221±116	5.33	> 0.05
Right	305±94	255±89	211±109	6.56	> 0.05
Cingulate gyrus					
Left	504±54	487±96	443±71	4.11	> 0.05
Right	559±84	499±108	456±94	4.45	> 0.05
SLF					
Left	1,094±112	980±116	546±111 [#]	10.11	< 0.05
Right	1,123±113	1,021±128	689±144 [#]	9.45	< 0.05
ALIC					
Left	947±104	854±118	1,843±233 [#]	7.33	< 0.05
Right	1,237±184	799±114	311±126 [#]	8.45	< 0.05
PLIC					
Left	2,047±129	1,843±233	867±118 [#]	12.65	< 0.05
Right	2,137±238	1,753±247	999±167 [#]	11.23	< 0.05
IFOF					
Left	109±45	97±48	88±30	3.19	> 0.05
Right	119±33	87±35	65±23	4.65	> 0.05
Thalamus					
Left	406±78	332±110	329±20	4.77	> 0.05
Right	521±195	355±113	313±63	3.61	> 0.05

Data are expressed as the mean ± SD, and analyzed by *F*-test. [#]*P* < 0.05, vs. moderate HIE group. SLF: Superior longitudinal fasciculus; ALIC: anterior limbs of internal capsule; PLIC: posterior limbs of internal capsule; IFOF: inferior fronto-occipital fasciculus; HIE: hypoxic-ischemic encephalopathy.

Table 6 Correlation between FA value and NBNA scores in different brain areas

Brain area	<i>r_s</i>	<i>P</i>
Corticospinal tract	0.478	< 0.05
Cingulate gyrus	0.460	< 0.05
SLF	0.311	> 0.05
ALIC	0.271	> 0.05
PLIC	0.646	< 0.01
IFOF	0.231	> 0.05
Thalamus	0.481	< 0.05

r_s: Correlation coefficient; SLF: superior longitudinal fasciculus; ALIC: anterior limbs of internal capsule; PLIC: posterior limbs of internal capsule; IFOF: inferior fronto-occipital fasciculus.

with Pearson correlation analysis. Receiver operating characteristic (ROC) curves were used to evaluate FA values in predicting the sensitivity and specificity of the prognosis in HIE children. A value of *P* < 0.05 was considered statistically significant.

Results

DTI parameters in normal, moderate and severe HIE patients

The ADC values in normal, moderate and severe HIE pa-

Table 5 Tract numbers in different brain areas of normal, moderate, and severe HIE patients

	Control (n = 10)	Moderate HIE (n = 14)	Severe HIE (n = 8)	F	P
Cingulate gyrus					
Left	245±72	225±52	145±62 [#]	4.31	< 0.05
Right	405±94	365±114	185±84 [#]	5.54	< 0.05
Corticospinal tract					
Left	494±54	444±84	334±67	13.22	> 0.05
Right	209±84	219±94	188±84	14.11	> 0.05
Thalamus					
Left	23±12	22±11	23±14	9.88	> 0.05
Right	187±31	134±33	145±54	9.12	> 0.05
ALIC					
Left	245±62	295±77	145±62	7.45	> 0.05
Right	685±84	585±112	455±68	8.88	> 0.05
PLIC					
Left	284±112	234±67	114±67 [#]	4.98	< 0.05
Right	988±233	678±234	188±84 [#]	5.44	< 0.05
IFOF					
Left	33±12	49±22	26±19 [#]	3.12	< 0.05
Right	156±39	197±33	112±33 [#]	4.33	< 0.05
SLF					
Left	225±52	155±72	56±15 [#]	4.12	< 0.05
Right	165±74	125±114	23±12 [#]	3.87	< 0.05

Data are expressed as the mean ± SD, and analyzed by *F*-test. [#]*P* < 0.05, vs. moderate HIE group. SLF: Superior longitudinal fasciculus; ALIC: anterior limbs of internal capsule; PLIC: posterior limbs of internal capsule; IFOF: inferior fronto-occipital fasciculus; HIE: hypoxic-ischemic encephalopathy.

tients were not significantly different (*P* > 0.05; **Table 2**).

FA values in the posterior limbs of the internal capsules and in the thalami showed statistically significant differences between the moderate and severe HIE groups (*F* value respectively 5.18/5.55 4.12/5.11 *P* < 0.05), and were significantly different between the control and moderate groups (*P* < 0.05; **Table 3**).

Voxel volumes in the superior longitudinal fasciculi, posterior limbs of the internal capsules and anterior limbs of the internal capsules showed statistically significant differences between the moderate and severe HIE groups (*P* < 0.05). There was no statistically significant difference between the control and moderate HIE groups (*P* > 0.05; **Table 4**).

DTT parameters in normal, moderate, and severe HIE patients

The fiber numbers in the posterior limbs of the internal capsules, cingulate gyri, superior longitudinal fasciculi and inferior fronto-occipital fasciculi were significantly different between the moderate and severe HIE groups (*P* < 0.05), but not significantly different between the control and moderate HIE groups (*P* > 0.05; **Table 5**, **Figure 1**).

Correlation between FA value and NBNA scores

All 10 cases of the control group had an NBNA score ≥ 35; the moderate HIE group included 3 cases scoring < 35, and

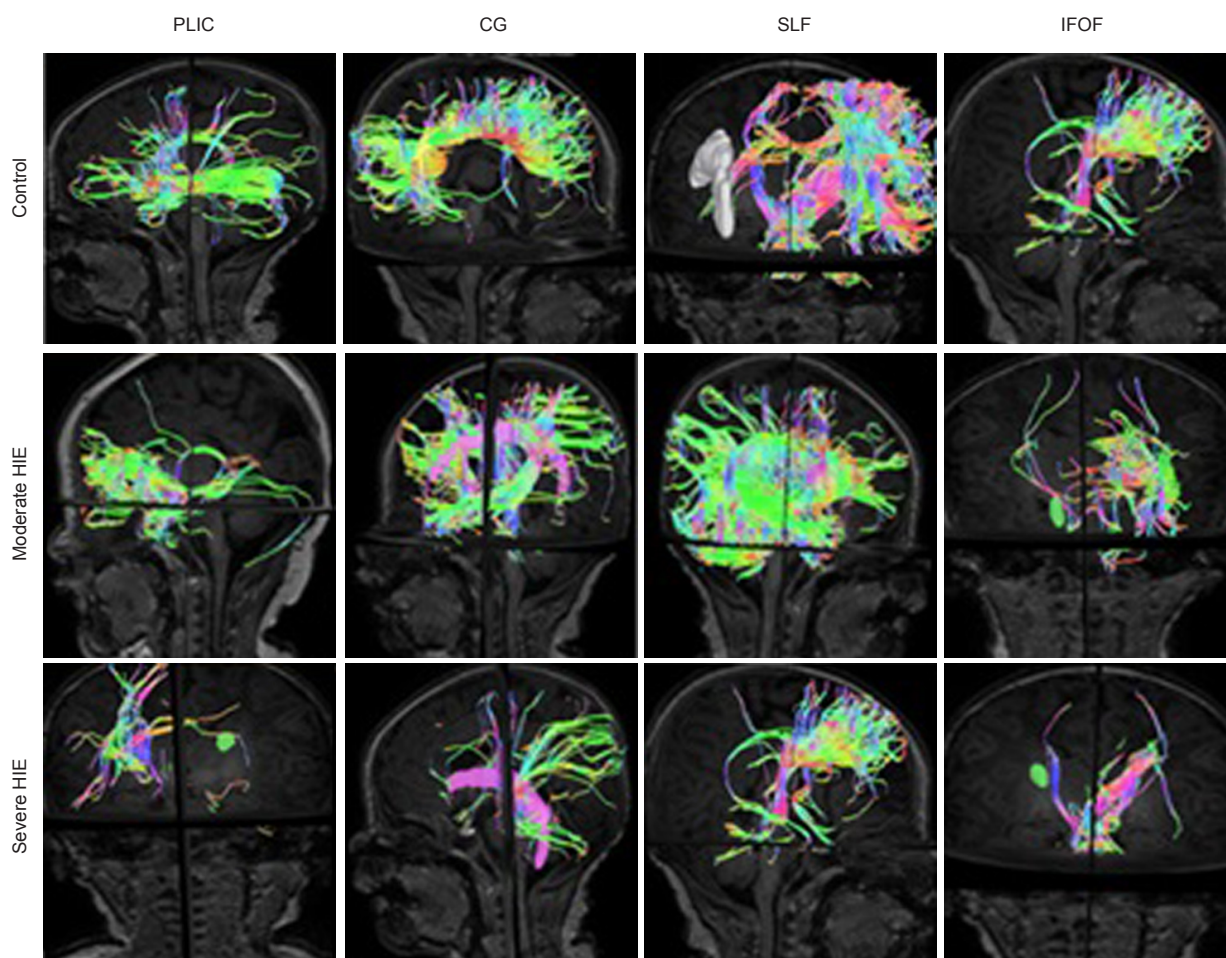


Figure 1 Diffusion tensor tractography of a normal infant, a moderate HIE infant and a severe HIE infant.

PLIC: Posterior limbs of internal capsule (green); CG: cingulate gyrus (purple); SLF: superior longitudinal fasciculus (green); IFOF: inferior fronto-occipital fasciculus (purple); HIE: hypoxic-ischemic encephalopathy.

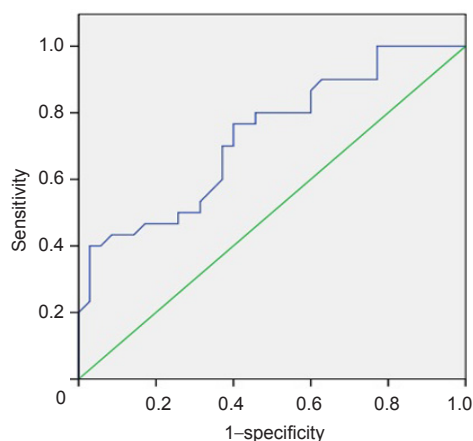


Figure 2 Receiver operating characteristic curve of diagnosis in posterior limb of internal capsule fractional anisotropy values and neonatal neurological assessment scores.

The area under the receiver operating characteristic curve (AUC) of fractional anisotropy values in anterior limbs of internal capsules is 0.779 ($P = 0.006$). The normal AUC value is between 1.0 and 0.5. In the case of $AUC > 0.5$, AUC is close to 1, to diagnose the better results. AUC in 0.5–0.7 with low accuracy, AUC in 0.7–0.9 with a certain accuracy, AUC in higher accuracy at above 0.9. The $AUC = 0.5$, no diagnostic value.

11 cases scoring ≥ 35 ; in the severe HIE group, all NBNA scores were < 35 (31.1 ± 1.6). *F*-test results showed that NBNA scores were significantly different among the three groups, with the severe HIE group having the lowest scores ($P < 0.01$). The correlation coefficient in the posterior limbs of the internal capsules was 0.646, higher than in other areas by Pearson relative analysis (Table 6).

The area under the ROC curve of FA values in the anterior limbs of the internal capsules was 0.779 ($P = 0.006$), using NBNA scores ≥ 35 as a good outcome. FA values (≥ 0.395) in the posterior limbs of the internal capsules predicted a good outcome and the corresponding sensitivity and specificity was 70.2% and 79.5%, respectively (Figure 2).

Discussion

There were no significant differences in ADC values among the different groups, which was consistent with a previous study (van Laerhoven et al., 2013). ADC values are important in the early diagnosis of HIE, and show pseudo-normalization after the acute stage (Winter et al., 2007). Guo et al. (2016) reported that within one week after birth, DWI used to detect ADC values demonstrated that the HIE sensitivity

was 83%, specificity was 63% and positive predictive value was 83%. However, patients in the acute stage possibly had severe lesions and unstable vital signs in each group. MRI examination was difficult to conduct in the acute phase (Li et al., 2014). HIE enters the subacute stage 1–3 weeks after birth. Studies have demonstrated that the diagnostic value of ADC values in the subacute stage is significantly decreased (de Vries et al, 2011). Our results verified that the FA values had a high diagnostic value. In particular, FA values were remarkably decreased in the dense white matter, splenium of the corpus callosum, and posterior limbs of the internal capsules. Significant differences in FA values were detected between the case and control groups. Currently, it is thought that decreased FA values are linked to cell death and loss of structural components of white matter fibers. Rutherford et al. (1998) reported that apoptosis was more obvious than necrosis in children in the subacute stage of HIE, which could explain why FA values decreased, but ADC values were normal. In this study, MRI in two cases of moderate HIE children revealed symmetric high-signal intensity in the thalami, without associated visible white matter damage; however, FA values were dramatically reduced in the thalami. This kind of basal ganglia/thalamus injury could cause athetoid cerebral palsy (de Vries et al., 2011). and indicates the possibility of severe cognitive impairment (Li et al., 2016b).

This has important clinical significance for early intervention (Dopwell et al., 2017). This report also analyzed the voxel volume. It is reported that a low voxel volume represents a severe injury. Conventional MRI T1WI and T2WI of the patients with severe HIE also showed damage in the thalami and basal ganglia. We found that voxel volume in various regions was significantly lower in the severe HIE group than in the moderate HIE group, especially in the thalami and heads of the caudate nuclei, suggesting serious motor impairment in the severe HIE group, which is consistent with the findings from a study by Lee et al. (2012b) concerning hypoxic-ischemic brain injury in adults.

The fiber numbers in the corticospinal tracts, inferior fronto-occipital fasciculi, anterior limbs of the internal capsules, and thalami were significantly different between the moderate and severe HIE groups, but were not significantly different between the control and moderate HIE groups. The injury to the integrity of white matter fibers means that the corresponding function may be affected. For example, corticospinal tract damage will affect motor function of the limbs. The superior longitudinal fasciculi, inferior longitudinal fasciculi, and frontooccipital fasciculi belong to long association fibers in the cerebral cortex and connect various areas of the cerebral cortex, so their injuries may affect cognitive, sensory, and motor functions. The inferior longitudinal fasciculi and frontooccipital fasciculi were damaged in the mild and moderate HIE groups, mainly affecting the temporal lobe and occipital lobe, and auditory, olfactory, taste, and language centers (Li et al., 2016a). Nevertheless, the corticospinal tract was the chief site of damage in the severe HIE group, affecting motor

function. This is matched with deductible item of NBNA scores and has some guiding significance for the evaluation of prognosis.

Correlation between FA values and NBNA scores in the moderate and severe HIE groups demonstrated that the rank correlation coefficient r_s of FA values and NBNA scores in the posterior limbs of the internal capsules was higher than that in the other regions. This may be associated with closely arranged white matter fibers, white matter fibers arranged in parallel, myelination at birth, and are easily detected by DTI after injury (Li et al., 2015). Moreover, these locations contain important white matter projection fibers associated with neuromotor function, and the anatomical location is easy to identify and measure. However, we did not obtain a threshold with a high sensitivity and specificity, which is possibly associated with the small sample size.

In summary, FA values, voxel volume, and number of fiber bundles in some ROIs quantitatively reflected white matter injury in neonates with HIE. The changes in DTI parameters were most obvious in the posterior limbs of the internal capsules, and may allow accurate and objective assessment of the degree of white matter injury in children with HIE. Among these parameters, the FA values in the posterior limbs of the internal capsules closely correlated with NBNA scores. DTI can be carried out in a single individual, so it has important clinical significance, and can accurately and objectively assess the prognosis.

Declaration of patient consent: *The authors certify that they have obtained all appropriate patient consent forms. In the form the patients have given their consent for their images and other clinical information to be reported in the journal. The patients understand that their names and initials will not be published and due efforts will be made to conceal their identity, but anonymity cannot be guaranteed.*

Author contributions: *XF contributed to definition of intellectual content of this topic and paper review. HXL was responsible for literature retrieval and designed the study. QW prepared and edited the paper. HXL, XD, MY and WJT participated in data acquisition. HXL, XF and QW were in charge of data analysis. MY did statistical analysis. All authors approved the final version of the paper.*

Conflicts of interest: *None declared.*

Plagiarism check: *This paper was screened twice using CrossCheck to verify originality before publication.*

Peer review: *This paper was double-blinded and stringently reviewed by international expert reviewers.*

References

- AbdelAziz NH, AbdelAzeem HG, Monazea EM, Sherif T (2017) Impact of thrombophilia on the risk of hypoxic-ischemic encephalopathy in term neonates. *Clin Appl Thromb Hemost* 23:266-273.
- Aridas JD, Yawno T, Sutherland AE, Nitsos I, Ditchfield M, Wong FY, Fahey MC, Malhotra A, Wallace EM, Jenkin G, Miller SL (2014) Detecting brain injury in neonatal hypoxic ischemic encephalopathy: Closing the gap between experimental and clinical research. *Exp Neurol* 261:281-290.
- Baldoli C, Scola E, Della Rosa PA, Pontesilli S, Longaretti R, Poloniato A, Scotti R, Blasi V, Cirillo S, Iadanza A, Rovelli R, Barera G, Scifo P (2015) Maturation of preterm newborn brains: a fMRI-DTI study of auditory processing of linguistic stimuli and white matter development. *Brain Struct Funct* 220:3733-3751.
- Bao XL (1995) Neonatal Behavior and Education of 0–3 Years Old. Beijing: China Children Publishing Press.

- Cavalleri F, Lugli L, Pugliese M, D'Amico R, Todeschini A, Della Casa E, Gallo C, Frassoldati R, Ferrari F (2014) Prognostic value of diffusion-weighted imaging summation scores or apparent diffusion coefficient maps in newborns with hypoxic-ischemic encephalopathy. *Pediatr Radiol* 44:1141-1154.
- Coleman MB, Glass P, Brown J, Kadom N, Tsuchida T, Scafidi J, Chang T, Vezina G, Massaro AN (2013) Neonatal neurobehavioral abnormalities and MRI brain injury in encephalopathic newborns treated with hypothermia. *Early Hum Dev* 89:733-737.
- de Vries LS, van Haastert IC, Benders MJ, Groenendaal F (2011) Myth: cerebral palsy cannot be predicted by neonatal brain imaging. *Semin Fetal Neonatal Med* 16:279-287.
- Dopwell F, Maypole J, Sinha B, Currier H, DeBassio W, Augustyn M (2017) "More than Meets the Eye": When the neonatal course may impact several years out. *J Dev Behav Pediatr* 38 Suppl 1:S44-S46.
- Duong TQ, Watts LT (2016) A brief report on MRI investigation of experimental traumatic brain injury. *Neural Regen Res* 11:15-17.
- Guo L, Wang D, Bo G, Zhang H, Tao W, Shi Y (2016) Early identification of hypoxic-ischemic encephalopathy by combination of magnetic resonance (MR) imaging and proton MR spectroscopy. *Exp Ther Med* 12:2835-2842.
- Hüppi PS, Dubois J (2006) Diffusion tensor imaging of brain development. *Semin Fetal Neonatal Med* 11:489-497.
- Jose A, Matthai J, Paul S (2013) Correlation of EEG, CT, and MRI brain with neurological outcome at 12 months in term newborns with hypoxic ischemic encephalopathy. *J Clin Neonatol* 2:125-130.
- Kim JH, Kwon YM, Son SM (2015) Motor function outcomes of pediatric patients with hemiplegic cerebral palsy after rehabilitation treatment: a diffusion tensor imaging study. *Neural Regen Res* 10:624-630.
- Krishnan P, Shroff M (2016) Neuroimaging in neonatal hypoxic ischemic encephalopathy. *Indian J Pediatr* 83:995-1002.
- Lee AY, Shin DG, Park JS, Hong GR, Chang PH, Seo JP, Jang SH (2012) Neural tracts injuries in patients with hypoxic ischemic brain injury: diffusion tensor imaging study. *Neurosci Lett* 528:16-21.
- Li HX, Tu WJ, Gao M, Jiang KH, Dong X (2014) Application research of resting state functional magnetic resonance imaging in newborn brain damage. *Zhonghua Shiyong Erke Linchuang Zazhi* 29:386-389.
- Li HX, Feng X, Tu WJ, Gao M, Jiang KH, Dong X (2016a) Application of resting state functional MRI in children with central nervous and psychological diseases. *Zhongguo Shiyong Erke Zazhi* 31:150-154.
- Li HX, Wang Q, Tu WJ, Gao M, Jiang KH, Lu YJ, Dong X (2015) Application of magnetic resonance diffusion tensor imaging technology in neonates with hypoxic-ischemic encephalopathy in the subacute stage. *Zhonghua Shiyong Erke Linchuang Zazhi* 30:1868-1872.
- Li XY, Tang ZC, Sun Y, Tian J, Liu ZY, Han Y (2016b) White matter degeneration in subjective cognitive decline: a diffusion tensor imaging study. *Oncotarget* 7:54405-54414.
- Okumura A, Hayakawa M, Tsuji T, Naganawa S, Watanabe K (2008) Diffusion tensor imaging in infants with basal ganglia-thalamic lesions. *Eur J Paediatr Neurol* 12:412-416.
- Pfefferbaum A, Rosenbloom MJ, Chu W, Sassoon SA, Rohlfing T, Pohl KM, Zahr NM, Sullivan EV (2014) White matter microstructural recovery with abstinence and decline with relapse in alcohol dependence interacts with normal ageing: a controlled longitudinal DTI study. *Lancet Psychiatry* 1:202-212.
- Pfister RH, Soll RF (2010) Hypothermia for the treatment of infants with hypoxic-ischemic encephalopathy. *J Perinatol* 30 Suppl:S82-87.
- Rutherford MA, Pennock JM, Counsell SJ, Mercuri E, Cowan FM, Dubowitz LM, Edwards AD (1998) Abnormal magnetic resonance signal in the internal capsule predicts poor neurodevelopmental outcome in infants with hypoxic-ischemic encephalopathy. *Pediatrics* 102:323-328.
- The Subspecialty Group of Neonatology Pediatric Society Chinese Medical Association (2005) Diagnostic criteria for neonatal hypoxic-ischemic encephalopathy. *Zhonghua Erke Zazhi* 43:584.
- van Laerhoven H, de Haan TR, Offringa M, Post B, van der Lee JH (2013) Prognostic tests in term neonates with hypoxic-ischemic encephalopathy: a systematic review. *Pediatrics* 131:88-98.
- Winter JD, Lee DS, Hung RM, Levin SD, Rogers JM, Thompson RT, Gelman N (2007) Apparent diffusion coefficient pseudonormalization time in neonatal hypoxic-ischemic encephalopathy. *Pediatr Neurol* 37:255-262.

Copyedited by Yu J, Li CH, Qiu Y, Song LP, Zhao M